NOTES AND CORRESPONDENCE

Variations in Near-Global Sea Level Pressure: Another View

TIM P. BARNETT

Climate Research Group, Scripps Institution of Oceanography, A-024, La Jolla, California

10 June 1987 and 5 October 1987

ABSTRACT

The behavior of large-scale patterns of sea level pressure is documented using a simple composite analysis over the period 1951–85. One interpretation of the maps shows that anomalies of a given sign appear sequentially along a closed, counterclockwise trajectory that transits Asia, eastward through the tropics of the Indo-Pacific then into the eastern Pacific, and finally back to Asia via the North Pacific. A typical time scale for this process is approximately 2 yr. Unfortunately, the composites are noisy and often poorly defined, thus allowing alternate interpretations.

1. Introduction

In a previous paper, Barnett (1985; hereafter B) described the existence of a large-scale moving sea level pressure (SLP) signal that included variability previously associated with the Southern Oscillation (SO), the monsoon systems in southeast Asia, and tropical–midlatitude teleconnection patterns. It was suggested that the moving SLP signal excited a natural mode of climate variability that had a preferred spatial pattern, i.e., the interaction of the moving disturbance and a standing wave. The above results were obtained from a complex empirical orthogonal function (CEOF) analysis on a near-global sea level pressure dataset. Extensive comparisons were made between the CEOF reconstructions and raw data to demonstrate the reality of the result. Yet the CEOF analysis is not particularly transparent, nor a perfect analysis tool. The sole purpose of the present note is to reexamine the SLP dataset with a far simpler, almost trivial, methodology to demonstrate that the features found by B are reproducible, although not irrefutably.

The primary results described by B have been confirmed by other workers. For instance, Yasunari (1985; 1987a,b) demonstrated the existence of eastward-moving features in heavily filtered SLP and zonal wind fields. His results also suggested the importance of climate variations over Asia in the global mode described above. The datasets he used were different than those used by B, as was his analysis technique. Meehl (1987) noted similar features in the unfiltered tropical surface station data and interpreted the apparent eastward movement as a local enhancement of the annual cycle associated with seasonal convection in the Indian–Pacific region. Kiladis and van Loon (1987) support and substantially elaborate on this finding. Recently, Gutzler and Harrison (1987), using upper-air station data, have also documented the existence of a moving signal that seems to originate in the eastern Indian Ocean although they note exceptions to this conclusion. Graham et al. (1987a,b), using an extended EOF analysis on both wind data within ±30° of the equator and a near-global SLP field, also document the existence of a moving anomaly pattern. Wright et al. (personal communication) performed extensive correlation studies with COADS data which show the eastward propagation in the SLP field although the motion does not appear to be either steady or dependable in their analysis.

Other recent work does not agree completely with the results discussed above. For instance, in a series of papers, van Loon and Shea (1985, 1987), examining variations of sea level pressure in the Southern Hemisphere associated with the Southern Oscillation, conclude that the large anomalies of sea level pressure form well ahead of that in the Northern Hemisphere. This observation, together with the large anomalies in the region of Australia and the South Pacific, suggests to them that the origins of the Southern Oscillation must be sought in that region (van Loon and Shea, 1985, 1987). However, the eastward propagation of signals across Australia from the Indian Ocean is apparent in their results (cf. their Figs. 1c–h of the 1987 paper). In a separate study, Trenberth and Shea (1987) investigate the cross correlation between SLP at various stations in the Indian and South Pacific regions. They also clearly demonstrate the eastward propagation of information in both the Indo-Pacific and Pacific lobes of the Southern Oscillation. However, they conclude that the signals originate in the South Pacific convergence

Corresponding author address: Dr. Tim P. Barnett, Climate Research Group A-024, Scripps Institute of Oceanography, University of California, San Diego, La Jolla, CA 92023.

zone (SPCZ) region. It is against this background of diverse ideas regarding the movement and origin of large climate anomalies that the current note is offered.

2. Data and analysis methods

The dataset used here is the near-global, sea level pressure field described in B. The data generally come from the products of national meteorological centers. In the equatorial strip, ship and island observations were used to complete the near global field. Observations south of 40°S are sparse and the data from this region should be considered unreliable. The dataset begins in January 1951 and extends monthly through 1986. It will be composited relative to warm events associated with ENSO.

Prior to analysis, the raw data were processed as follows: long-term monthly means at each grid point were computed and subtracted, leaving a monthly anomaly field relative to a 35-year mean. Seasonal averages of this monthly data were subsequently formed. Finally, and perhaps most importantly, each gridded time series was normalized by its own standard deviation. This is a significant departure from the procedure followed by van Loon and Shea (1987). However, it is necessary if one wishes to investigate the role of both the equatorial and high-latitude regions in SLP variability since the variance is appreciably smaller in the tropics than at high latitudes. The result of the above operations is a very lightly processed dataset which was then submitted to composite analysis.

The warm events to be composited used year_0 definitions from Table 1 of van Loon and Shea (1985). Given the length of the present dataset, plus the fact that we wish to extend into the year prior to year_0 meant that a total (N) of eight events could be studied (1953, 1957, 1963, 1965, 1969, 1972, 1976, 1982). The composites were computed from the year before to the year after a warm event, i.e., 12 seasons. Define $P_i(\mathbf{x}, \nu)$ to be the normalized pressure field at position $\mathbf{x}$ for season ν and warm event i where $\nu = 1, 2, \cdots, 12$ and $i = 1, 2, \cdots, 8$. Then the composite for a particular location/season is formed as follows:

$$\bar{P}(\mathbf{x}, \nu) = \frac{1}{N} \sum_{i=1}^{N} P_i(\mathbf{x}, \nu).$$

The composites will be presented in their normalized form so as to obtain an idea of the variability *between* events. Thus, we define the standard deviation between composites as

$$\sigma = \left[\frac{\sum_i (P_i - \bar{P})^2}{N - 1} \right]^{1/2}.$$

The final normalized composite maps are denoted by P' where

$$P'(\mathbf{x}, \nu) = \frac{\bar{P}(\mathbf{x}, \nu)}{\sigma(\mathbf{x}, \nu)}.$$

Thus, P' has the sign of the composite averaged anomaly and a magnitude that is like a t-statistic.

3. Results

The normalized composites are shown in Figs. 1–3. It is immediately clear that the typical signal strength of the composite is low (e.g., the 0.05 significance level is 2.3). This means that the individual numbers shown on the composite maps are generally meaningless. What is impressive about the maps, however, is the large spatial scale of anomalies of like sign and the fact that these anomalies transcend boundaries between different datasets used to form the global SLP field. This, plus the strong continuity in time shown by the composites, suggests that they are indeed representing real features of the atmosphere. The relatively small standardized values mean that there is a large amount of variability between the different warm events. In fact, the numbers suggest that the event-to-event variability is larger than the average of a typical event. Thus, the composite maps provide a useful qualitative description of warm events but one that should not be trusted in detail. (See, also, Trenberth and Shea, 1987.) This means attempts to connect successive regions of, say, largest positive anomalies are apt to be misleading and ambiguous. Rather, it is necessary to view the disposition of large regions of like-sign anomaly.

In the year *before* a warm event (Fig. 1), much of Asia is covered by lower than normal pressure. As the year progresses, the low-pressure anomalies intensify and are displaced from Southeast Asia eastward into the Pacific. By the end of the year, the low pressure over Asia has virtually disappeared and is now replaced by high pressure that appears linked to similar anomalies over the midlatitude Pacific. The other main feature of Fig. 1 is the intensification of high-pressure anomalies in the eastern Pacific during the first three-quarters of the year. This combination of highs and lows represents one phase of the Southern Oscillation. During SON_{-1}, the center of the high pressure anomaly is displaced north of the equator and we see the beginnings of a "wrap around" of the anomaly into Asia, although this feature, seen also by B, Yasunari (1987b) and Kiladis and van Loon (1987), is associated with high noise levels in the composites. If one tries to follow the displacement of the highest anomalies then many interpretations of Fig. 1 are possible. However, the data do not justify such a microscopic view for the reasons noted above.

During the year of a warm event (Fig. 2), high pressure has expanded westward and southward from the previous year so that it now covers the entire Asian continent and Indo-Pacific at the beginning of the year. As we saw above, this region of high pressure intensifies as the year progresses and the region of maximum pressure anomaly moves from the Indian subcontinent to over Indonesia. The low pressure that had occupied

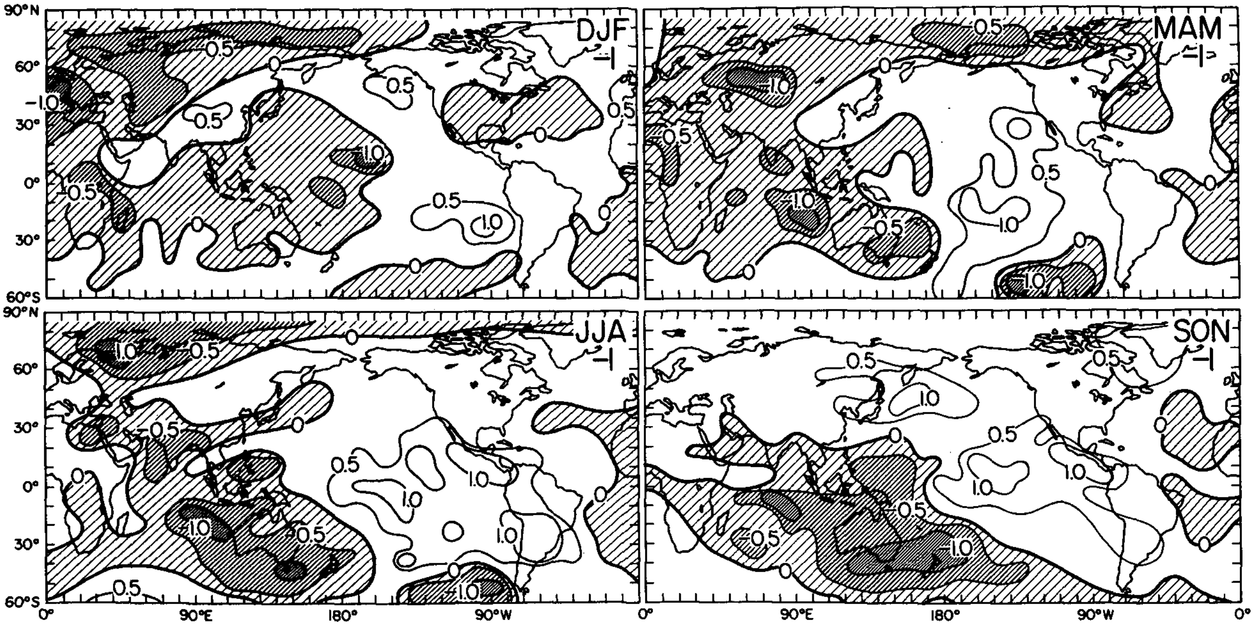

FIG. 1. Composite seasonal anomaly maps for the year before warm events. The values shown are the composite normalized by the standard deviation between composites.

the Indian Ocean during the preceding year is seen to be sequentially displaced eastward into the Pacific. During December, January, February [DJF_0], the negative anomaly is exceptionally weak and appears as a dipole about the equator. As the year wears on, that feature moves eastward and rapidly expands until it covers the entire eastern and north Pacific by the northern summer. The amplification in the last half of $year_0$ suggests an intensification of a standing wave, for there is little change of position of anomalies in the equatorial band between the two seasons. At higher latitudes, however, the "wrap-around" effect appears

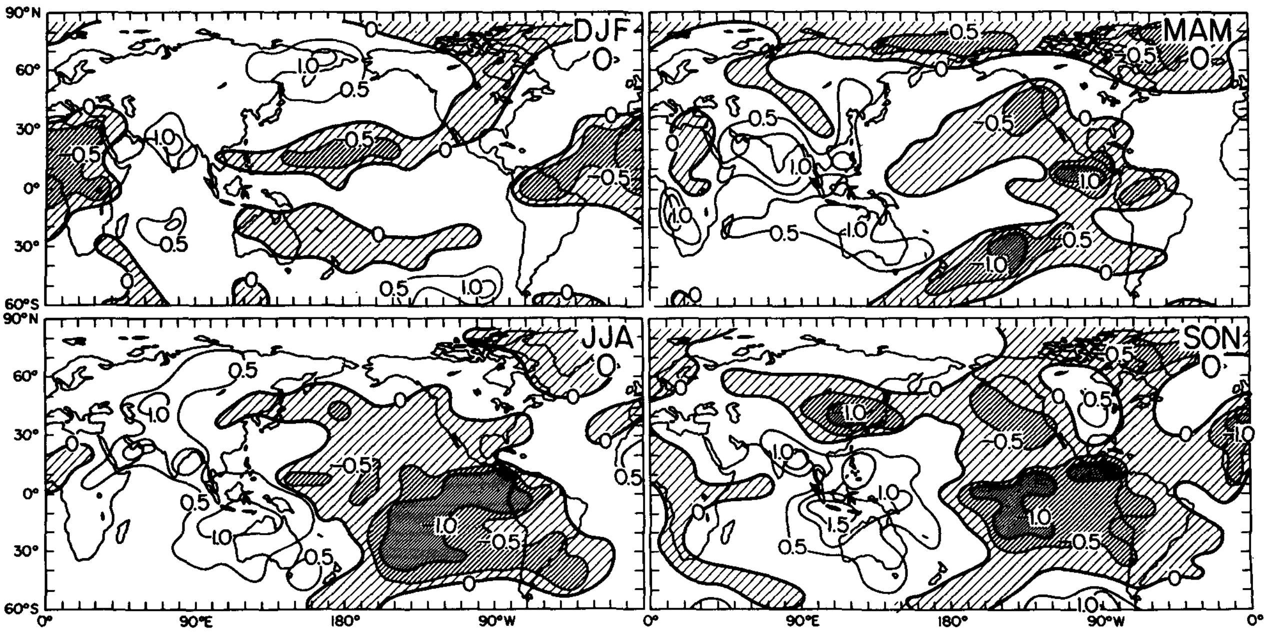

FIG. 2. As in Fig. 1 except for the year of the warm event.

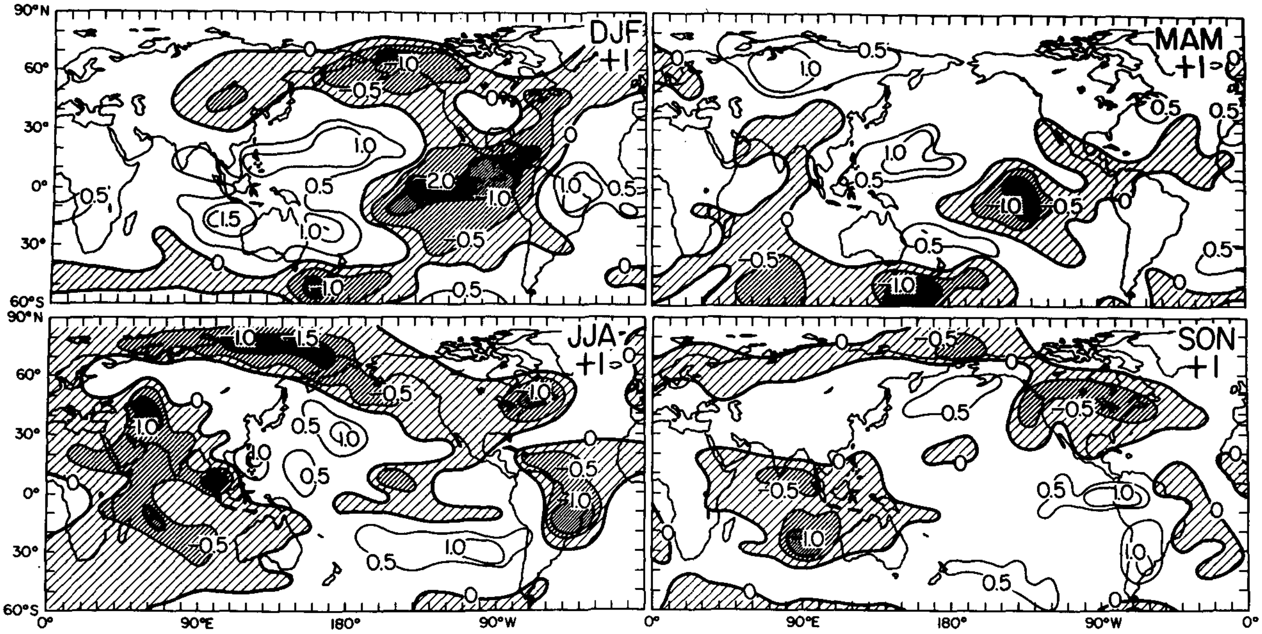

FIG. 3. As in Fig. 1 except for the year after the warm event.

to be taking place [SON_0] although again, the signal is not strong.

During $year_{+1}$ (Fig. 3), the high-pressure anomaly that was over Indonesia and Australia is seen to be sequentially displaced eastward into the Pacific, bifurcating about the equator and rapidly losing amplitude by the end of the year. A semblance of a PNA pattern is seen but it is not as clear as in nonstandardized studies (cf. van Loon, 1986). The "wrap around" of the low-pressure anomaly that began in the preceding year continues but soon becomes weak and difficult to follow. For instance, there is an abrupt hiatus in the event over Asia (even a change of sign of the anomaly) in $(MAM)_{+1}$. By the end of the $year_{+1}$, the anomaly (low pressure in this case) that once covered most of Asia appears to take a position west of Australia. But the composites are confusing as to whether the signal moved from Asia or the South Indian Ocean.

The sequence of patterns shown in Figs. 1–3 are virtually identical to those described by Barnett (1985). While "propagation" is perhaps not a proper description of what is happening, it is abundantly clear that the main centers of the anomaly activity undergo horizontal translations. The main zonal translation occurs from India to the coast of South America. The meridional translation appears over Asia and in the eastern Pacific and can also be thought of as familiar teleconnection patterns.

The relation between individual patterns and their evolution can be quantified. Let us select the period JJA_{-1} as a convenient time mark and denote its seasonal index by ν_0. Subsequent results are not strongly affected by this choice. We next compute the pattern correlation between the composite JJA_{-1} and all other composite maps shown on Figs. 1–3, i.e.,

$$r = \frac{\langle P'(\mathbf{x}, \nu_0)P'(\mathbf{x}, \nu)\rangle_\mathbf{x}}{\langle [P'(\mathbf{x}, \nu_0)]^2\rangle_\mathbf{x}^{1/2}\langle [P'(\mathbf{x}, \nu)]^2\rangle_\mathbf{x}^{1/2}}, \quad \nu = 1, 2, \cdots, 12$$

where it is understood that $\langle P'\rangle_\mathbf{x} \equiv 0$.

The resulting pattern correlations are shown in Fig. 4. Also shown in Fig. 4 (insert) are the theoretical pattern correlations that would be expected if the events shown in Figs. 1–3 were the result of either a pure standing wave or a pure progressive wave. The actual pattern correlation appears to resemble more closely the shape expected theoretically from a purely progressive wave system. If noise were introduced to the theoretical analysis, however, the distinction might not be so clear.

The remarkable fact about Fig. 4 is the strength of the correlation between JJA_{-1} and JJA_0. The correlation is −0.59 and was computed using the *entire* global field. The correlations were also computed without regard to area weighting. If the highest latitudes and the Atlantic region, where there is little signal, were ignored, the correlation would be substantially stronger. In any event, the results of Fig. 4 indicate the global-scale SLP variation described here will, on average, largely run its course over an approximate 2-yr period (van Loon and Shea, 1985; Meehl, 1987).

4. Discussion

The simple composite analysis performed on data that is but lightly filtered reproduces the earlier findings

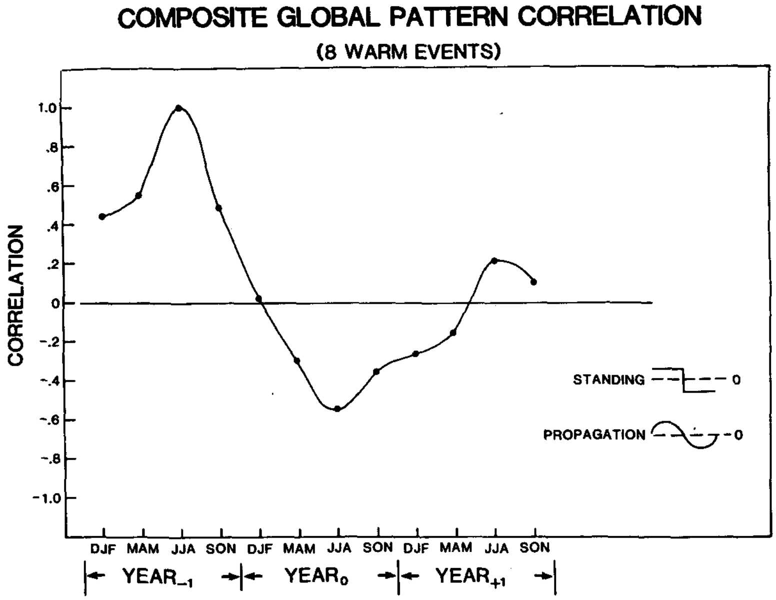

FIG. 4. Pattern correlation between the normalized composite map for JJA_{-1} and all other composites. The inset shows the theoretically expected signals if the composites represented a purely progressive or standing wave.

of B, Yasunari (1987b), Meehl (1987), Kiladis and van Loon (1987), and Graham et al. (1987b) and the suggestion of Gutzler and Harrison (1987). The link between Asia and the ENSO signal is relatively clear in the composites—much more clear than shown in B, for instance. The sequential eastward displacement of anomaly centers from the central Indian Ocean to the central Pacific is clear and seems to have been found in enough different studies with different data to be fairly firmly established. The intensification of a natural mode ("standing wave") is also clear during the $year_0$ of a warm event. Finally, the "back interaction" between anomalies in the midlatitude Pacific and those which subsequently develop over Asia is also suggested, but not unambiguously. This latter result was also noted by Yasunari (1985, 1987b), Kiladis and van Loon (1987), and Graham et al. (1987a) and appears to be an important aspect of the evolution of the SLP field. In summary, all of the main features found in the CEOF analysis are reproduced with the much more transparent calculations used here. Unfortunately, the compositing results in general are noisy and while supportive of the above scenario, hardly conclusive.

The details shown in the composite for the Southern Hemisphere also agree, in general, with those described by van Loon and Shea (1985, 1987). Since those authors did not weight the anomaly field by its variance, their results tend to concentrate on the higher latitudes of the Southern Hemisphere. Also, since they considered only the Southern Hemisphere below about 15°S, the connection between their results there and those in the equatorial and Northern Hemisphere regions was not apparent. In a separate study, van Loon (1986) did consider global SLP composites and, in general, obtained results just like many of those given above. Finally, the results shown here are entirely consistent with those of Trenberth and Shea (1987) wherein eastward displacement of anomalies is seen through both lobes of the traditional Southern Oscillation pattern.[1] All of the authors, however, interpret their results differently.

One of the difficulties with accepting the results given by B and section 3 is the connotation that may be associated with "progressive" wave phenomenon. Free waves of the time scale found here are not known to exist in the atmosphere. It therefore appears that the features must be forced. A likely explanation for the apparent motion of the anomaly centers, at least in the tropics, can be found in Meehl (1987) and to a lesser extent in the suggestions of Gutzler and Harrison (1987). Meehl particularly, shows that the center of maximum convection moves seasonally from the region of India in JJA to the southeast Pacific in MAM. The idea expressed by the above authors is that a low-frequency modulation of the amplitude of the seasonal cycle could explain some of the features seen above. This idea is elaborated upon in Kiladis and van Loon (1987). Such an explanation is attractive for it invokes seasonal cycle physics to give a major part of the tropical results shown in Figs. 1–3.

[1] Those authors make the important suggestion that the behavior of the SLP field shown above for the post-1950s may have been different in the period 1880–1940.

Acknowledgments. This work was supported by NSF Grant ATM85-13713. Useful discussions of these results with Harry van Loon, Kevin Trenberth, Jerry Namias and Nick Graham helped sharpen the ideas presented here. Rick Rosen was a great help in tuning the final draft.

REFERENCES

Barnett, T. P., 1985: Variations in near-global sea level pressure. *J. Atmos. Sci.,* **42,** 478–501.

Graham, N. E., J. Michaelsen and T. P. Barnett, 1987a: An investigation of the ENSO cycle with statistical models. Part I: Predictor Field Characteristics. *J. Geophys. Res.,* in press.

——, —— and ——, 1987b: An investigation of the ENSO cycle with statistical models. Part II: Model results. *J. Geophys. Res.,* in press.

Gutzler, D. S., and D. E. Harrison, 1987: The structure and evolution of seasonal wind anomalies over the near-equatorial eastern Indian and western Pacific Oceans. *Mon. Wea. Rev.,* **115,** 169–192.

Kiladis, G. N., and H. van Loon, 1987: The Southern Oscillation. Part VII: Meteorological anomalies over the Indian and Pacific sectors associated with the extremes of the oscillation. *Mon. Wea. Rev.,* in press.

Meehl, G. A., 1987: The annual cycle and interannual variability in the tropical Pacific and Indian Ocean regions. *Mon. Wea. Rev.,* **115,** 27–50.

Trenberth, K., and D. Shea, 1987: On the evolution of the Southern Oscillation. *Mon. Wea. Rev.,* in press.

van Loon, H., 1986: Characteristics of sea level pressure and sea surface temperature during the development of a warm event in the Southern Oscillation. *Namias Symposium,* J. O. Roads (Ed.), SIO Reference Series 86-17, 160–173. [Available from Scripps Institution of California, La Jolla, 92093.]

——, and D. Shea, 1985: The Southern Oscillation. Part IV: The precursors south of 15°S to the extremes of the Oscillation. *Mon. Wea. Rev.,* **113,** 2063–2074.

——, and ——, 1987: The Southern Oscillation. Part VI: Anomalies of sea level pressure on the Southern Hemisphere and of Pacific sea surface temperature during the development of a warm event. *Mon. Wea. Rev.,* **115,** 370–379.

Yasunari, T., 1985: Zonally propagating modes of the global east–west circulation associated with Southern Oscillation. *J. Meteor. Soc. Japan,* **63**(6), 1013–1029.

——, 1987a: Global structure of the El Niño/Southern Oscillation. Part I: El Niño composites. *J. Meteor. Soc. Japan,* **65,** 67–80.

——, 1987b: Global structure of the El Niño/Southern Oscillation. Part II: Time evolution. *J. Meteor. Soc. Japan,* **65,** 81–102.